

## PAPER

## Nitrogenated Aromatics from Chitin

Camila Souza Santos,<sup>†,a</sup> Renan Rodini Mattioli,<sup>†,a,b</sup> Julia Soares Baptista,<sup>a</sup> Vitor H. Menezes da Silva,<sup>a</sup> Duncan L. Browne<sup>b</sup> and Julio Cezar Pastre<sup>\*,a</sup>Received 00th January 20xx,  
Accepted 00th January 20xx

DOI: 10.1039/x0xx00000x

Herein, we addressed the challenge of using two chitin-derived furans, namely 3-acetamido-5-ethylfuran (**3A5EF**) and 3-acetamido-5-(1-hydroxyethyl)furan (**3A5HF**), for the formation of 4-acetylaminophthalimides and other *N*-containing aromatic compounds. The transformation is carried out sequentially and involves the formation of the Diels-Alder adduct, forming 7-oxa-norbornene backbone, which, in an acidic/acetylation medium, undergoes a dehydration/aromatisation process providing nitrogenated aromatic compounds in yields ranging from 16–80%. The preparation of 4-acetylaminophthalimides from a chitin derivative is the first step towards expanding the toolbox of chitin-derived furans in the synthesis of unique nitrogenated aromatic compounds with the nitrogen atom directly attached to the benzene ring.

## Introduction

Since the beginning of the chemical industry, aromatic compounds have played a crucial role in the production of high added-value chemicals and materials. Currently, fossil carbon sources (oil, coal and natural gas) are still the predominant starting materials for the synthesis of aromatic compounds, mainly produced from the naphtha fraction of crude oil (Figure 1a).<sup>1</sup> However, it is well known that high consumption of fossil resources associated with growing environmental concerns requires the identification of sustainable alternatives for obtaining fuels, chemicals and functional materials.<sup>2,3</sup> In this context, biomass presents itself as a promising and sustainable source of organic carbon, with great potential for substitution and supplementation of fossil resources accordingly to the fundamental principles of Green Chemistry.<sup>4</sup> Among the available biomasses, chitin is the second most abundant biopolymer in nature and the main constituent of the exoskeleton of arthropods. Although chitin occurs on a larger scale in arthropods, it also can be found in cell walls, fungi, yeast and some organisms in the lower plant and animal kingdoms.<sup>5</sup>

In recent decades, chitin has been used for several applications in the field of cosmetics, textiles, agriculture, biomedicine and water treatment.<sup>6</sup> In terms of annual production, chitin has numbers similar to cellulose and more than 100 billion tons are produced annually as crustacean shell waste generated by the global seafood industry. However, chitin still receives less attention when compared to lignocellulosic biomass.<sup>7</sup> Rapid growth in the global-population

has also pushed seafood aquaculture production increasing the availability of seafood waste and, thus, creating new opportunities to chitin-based biorefinery approaches.<sup>8</sup>

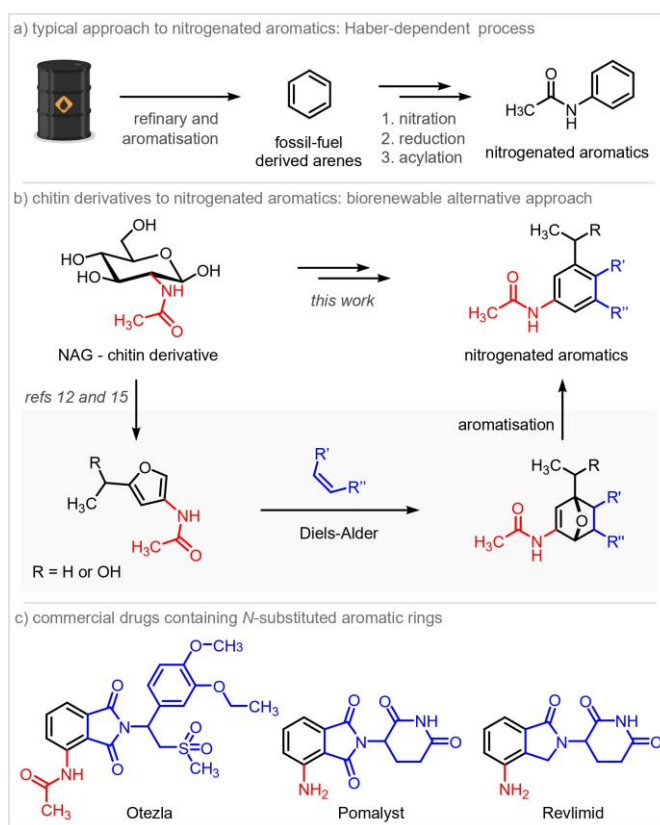


**Figure 1** Sustainable production of nitrogenated aromatic compounds from chitin-derived Diels-Alder adducts.

<sup>a</sup> Institute of Chemistry, University of Campinas (UNICAMP), 13083-970, Campinas, SP, Brazil. Email: jpastre@unicamp.br

<sup>b</sup> School of Pharmacy, University College London (UCL), WC1N 1AX, London, UK.

<sup>†</sup> These authors contributed equally to this work.

<sup>‡</sup> Electronic Supplementary Information (ESI) available: Experimental Procedures, NMR Spectrum, HRMS and FTIR (ATR) Data, Theoretical Model and Computational Methods. See DOI: 10.1039/x0xx00000x

The most common marine waste used to produce chitin is the cuticles of various crustaceans, mainly crabs and shrimps.<sup>9</sup> Conventionally, these raw materials pass through demineralisation and deproteinisation operational units

involving strong acids and bases and temperatures in the range of 100 °C or above to afford chitin on an industrial scale. These processes require high energy consumption and generate effluents to be neutralised.<sup>10</sup> Nonetheless, the chemical deproteinisation step can be replaced by enzymatic processes which avoids alkaline treatments and reduces energy, chemicals and water consumption.<sup>11</sup>

Chitin has a unique potential for obtaining nitrogen-containing derivatives, such as *N*-acetyl-D-glucosamine (NAG), D-glucosamine, *N*-acetylglycine (NAG), *N*-acetyl sorbitol, *N*-acetyl isosorbide, and 3-acetamido-5-acetylfuran (**3A5AF**).<sup>12</sup> This latter chemical is particularly valuable as it contains a substitution pattern that is difficult to synthetically install, representing a real opportunity for chemical valorisation.<sup>13–17</sup>

Recently, Pereira and co-workers developed a methodology for the preparation of Diels-Alder (DA) adducts using **3A5AF** as diene and a range of maleimides as dienophiles. Highlighting the positive effect of the *N*-acetyl substituent in the feasibility of the reaction, their methodology provided the adducts in good yields at the expense of using buffered systems and deuterated dimethyl sulfoxide.<sup>18</sup>

Several approaches to convert bio-derived intermediates into oxygenated aromatics have been presently explored in the last years. Among several options, the furan cycloaddition/aromatisation reaction approach stands out in terms of efficiency and versatility, allowing easy access to valuable scaffolds such as substituted benzenes, phthalic anhydride derivatives, phthalides and phthalimides.<sup>19–31</sup>

In this sense, the reactivity of furan derivatives as dienes has been the subject of numerous theoretical and experimental studies and the general consensus is that good kinetics and yields require electron-rich furans and activated dienophiles.<sup>21</sup> Moreover, DA reactivity is enabled by the chemical derivatisation of electron-poor furans, via reduction, hydration or hydrazone formation.<sup>22–31</sup> According to Frontier Molecular Orbital (FMO) theory, the [4+2] cycloaddition reaction is governed by the energy gap between the corresponding HOMO of the diene and the LUMO of the dienophile, although the activation barriers and thermodynamic stability of the adducts also play an important role in this chemistry.<sup>32</sup>

Major efforts on the furan DA/aromatisation chemistry have focused on lignocellulosic derived furans.<sup>33–40</sup> Although this led to significant achievements, the formation of relevant *N*-containing derivatives still relies on the introduction of the nitrogen atom before or after the DA reaction and using – but not limited to – reductive aminations.<sup>40b</sup> Nitrogen is undoubtedly important in modern medicine considering that over 80% of approved drugs contain at least one nitrogen atom.<sup>16,41</sup> However, the vast majority of nitrogen present in pharmaceuticals is sourced from ammonia, which is derived from the Haber process;<sup>42–44</sup> some representative examples being the drugs Otezla®, Pomalyst® and a Revlimid® analogue (Figure 1c). The Haber process consumes enormous amounts of energy due to the scale of global ammonia production and the harsh conditions required to break the strong *N–N* triple bond in nitrogen gas. Nevertheless, nature has evolved efficient nitrogenase enzymes that convert gaseous nitrogen into

ammonia, and subsequently, is incorporated into nitrogen-based building blocks that compose the biopolymers, e.g. chitin.<sup>16</sup> Thus, a sustainable alternative for the synthesis of *N*-compounds should employ readily available reservoir of biologically-fixed nitrogen as a source of this heteroatom.

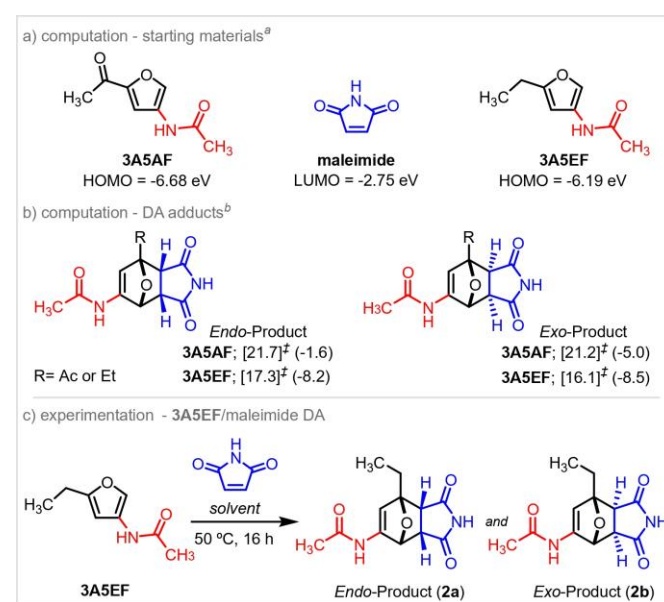
In this work, we developed a new method to produce high added-value aromatics using chitin-derived furans employing a tandem approach based on the DA reaction followed by the aromatisation step (Figure 1b). To the best of our knowledge, there are no reports in the literature for the formation of 4-acetylamino-phthalimides and other *N*-containing aromatic compounds derived from renewable sources.

## Results and discussion

### Diels-Alder reaction investigation of chitin-derived furans

We commenced our study by computationally analysing the reactivity of two chitin-derived furans, **3A5AF** and **3A5EF**, against the dienophile maleimide (**1**) by means of Density Functional Theory (DFT, see ESI† for details). Based on the HOMO energies depicted in Table 1a, **3A5EF** is more reactive than **3A5AF**. Indeed, the higher reactivity of **3A5EF** is reflected by considerably reduction of  $\Delta G^\ddagger$  comparing **3A5AF** with **3A5EF** (4.4 and 5.1 kcal/mol for *endo* and *exo* transition states, respectively). Moreover, the DA reaction for **3A5EF** has higher exothermicity than its counterpart DA reaction with **3A5AF**.

**Table 1** Scope of solvents for the DA reaction between **3A5EF** and maleimide (**1**)



Entry <sup>c</sup>	Solvent	Yield (%) <sup>d</sup>	Exo:Endo Ratio <sup>d</sup>
1	Methanol	87 (76) <sup>e</sup>	9:1
2	Ethanol	84	9:1
3	2-Propanol	88	7:1
4	Dimethylformamide	82	7:1
5	Dimethyl carbonate	77	3:1
6	Ethyl acetate	73	3:1
7	Methanol/2,2,2-Trifluoroethanol 4:1	98	6:1

8 Toluene/Methanol 9:1 84 4:1

<sup>a</sup> Calculated frontier molecular orbital for reactants. <sup>b</sup> Gibbs free energy activation barriers [ $\Delta G^\ddagger$ ] and reaction energies ( $\Delta G$ ) in solution-phase at 323.15 K are given in kcal/mol. Methanol was used for the implicit solvent model (see ESI<sup>†</sup> for details). <sup>c</sup> Reaction conditions: **3A5EF** (3.83 mg, 25  $\mu$ mol, 1.0 equiv.), **1** (2.43 mg, 25  $\mu$ mol, 1.0 equiv.), indicated solvent (1 mL, 25 mM). <sup>d</sup> Obtained using <sup>1</sup>H NMR analysis and 1,3,5-trimethoxybenzene as internal standard. <sup>e</sup> Isolated yield.

Based on the computational findings, we selected **3A5EF** as the diene to conduct the experimental investigation on the kinetics profile of the DA reaction. The kinetics experiment was performed under standard conditions (50 °C, 16 h, 1.0 equiv. of **3A5EF** and 1.2 equiv. of **1**).<sup>39</sup> According to Figure 2, it can be noted that the DA reaction goes to completion in ca. 4 h yielding 87% (sum of **2a** + **2b**), after that, accumulation of the *exo* isomer to the detriment of the *endo* isomer takes place. A clear plateau for the formation of the *exo* adduct could not be reached even after 16 h, however prolonged reaction times led to similar *exo:endo* selectivity at equal yields affording 9:1 for *exo:endo* product ratio.

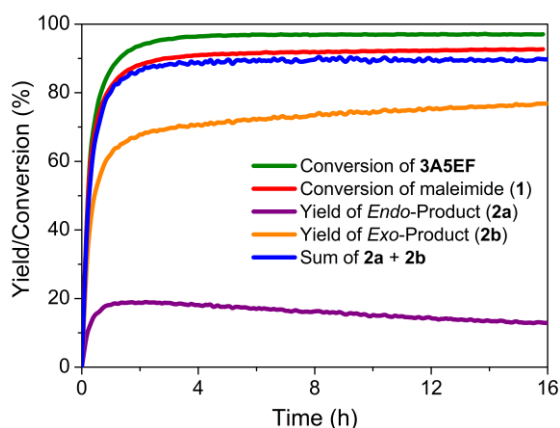


Figure 2 Kinetic profile for the reaction between **3A5EF** and maleimide (**1**).

The formation of the DA adducts **2a** and **2b** in good combined yield was carried out in a variety of solvents with different properties and origins, including green solvents. Table 1c shows the yields and *exo:endo* ratios obtained for the model reaction of this study (between **3A5EF** and **1**) at 50 °C for 16 h using selected solvents (for the complete set of solvents evaluated, see Table S1 in ESI<sup>†</sup>). Gratefully, based on the  $\Delta\Delta G^\ddagger$  obtained from Table 1b, the *exo:endo* product ratio is computed to be 7:1 in good agreement with the experimental ratio (Table 1c, entry 1). In general, most solvents investigated were efficient for DA adduct formation. The yields obtained showed little variation between them (on average 75%) and led to the formation of the *exo* adduct (**2b**) as the major product. Protic polar solvents such as methanol, ethanol, 2-propanol and a methanol/2,2,2-trifluoroethanol mixture (Table 1c, entries 1–3 and 7 respectively), resulted in the highest yields, while methanol and ethanol afforded the highest diastereoisomeric ratio (*exo:endo*). Thus, methanol was determined to be the best solvent for the formation of the DA adducts; the isolated product was obtained in 76% yield. Other reaction parameters

such as temperature (microwave irradiation or conventional heating) and use of Lewis acids as catalysts were also evaluated (see Tables S2–S4 in ESI<sup>†</sup> for details). Although a good compromise between time, temperature, yield, and selectivity could be observed, these conditions gave essentially the same results. In order to make the procedure as simple as possible, we selected the results obtained in methanol at 50 °C for 16 h as optimal.

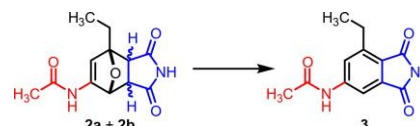
Beyond **3A5EF**, we also performed the formation of DA adducts using the other two chitin-derived furans of interest **3A5HF** and **3A5AF** (see Figures S12–S17 in ESI<sup>†</sup> for details) at optimal conditions in 53% (**2c** + **2d**, *exo:endo* ratio = 12:1) and 45% (**2e** + **2f**, *exo:endo* ratio = 5:1) combined yields, respectively. It is noteworthy that **3A5EF**-derived DA adducts **2a** and **2b** showed higher combined yield (76%) in comparison to two chitin-derived analogues. These results strengthen the use of **3A5EF** to further investigations.

### Aromatisation step optimisation

Facing well-established experimental conditions for the DA reaction with **3A5EF**, we turned our attention to the main objective of our work exploring the aromatisation reaction of the DA adducts. According to Table 2, we started the investigation using standard acidic conditions to promote the dehydration reaction, however the use of *p*-TsOH·H<sub>2</sub>O led to the formation of the ketone derivative **2g** (see Figure S18 in ESI<sup>†</sup> for details) *via* hydration of the double bond and acetamide elimination (Figure 3c). On the other hand, the use of a Dean-Stark apparatus (Table 2, entry 1) led to an unwanted competitive retro-DA reaction. We also verified that the adduct is poorly soluble in toluene, so we changed the solvent to THF and used 3 Å molecular sieves to avoid the formation of the ketonic by-product (Figure S18), however product **3** could not be observed. We tested the use of other acid catalysts such as Amberlyst-15 and sulphuric acid supported on silica (H<sub>2</sub>SO<sub>4</sub>-SiO<sub>2</sub>), but again these conditions did not lead to product **3** (Table 2, entries 3 and 4). Basic conditions using *t*-BuOK or DABCO were also investigated, but the DA adduct was not consumed under these conditions (Table 2, entries 5 and 6).

Table 2 Optimisation of experimental conditions for the aromatisation step

Entry <sup>a</sup>	Solvent	Ac <sub>2</sub> O (equiv.)	Acid or Base (equiv.)	Temperature, Time	Yield <sup>d</sup> (%)
1	PhMe	-	<i>p</i> -TsOH (0.5) <sup>b</sup>	110 °C, 15 h	-
2	THF	-	<i>p</i> -TsOH (0.5) <sup>c</sup>	50 °C, 15 h	-
3	THF	-	Amberlyst-15 (0.5) <sup>c</sup>	50 °C, 15 h	-
4	THF	-	H <sub>2</sub> SO <sub>4</sub> -SiO <sub>2</sub> (0.5) <sup>c</sup>	50 °C, 15 h	-
5	THF	-	<i>t</i> -BuOK (0.5) <sup>c</sup>	50 °C, 15 h	-
6	THF	-	DABCO (0.5) <sup>c</sup>	50 °C, 15 h	-
7	-	4	H <sub>2</sub> SO <sub>4</sub> (0.5)	50 °C, 10 h	80
8	-	4	H <sub>2</sub> SO <sub>4</sub> (0.5)	25 °C, 15 h	70



<b>9</b>	-	2	H <sub>2</sub> SO <sub>4</sub> (0.5)	50 °C, 10 h	50
<b>10</b>	-	4	H <sub>2</sub> SO <sub>4</sub> (0.25)	50 °C, 10 h	70
<b>11</b>	-	4	<i>p</i> -TsOH (0.5)	50 °C, 10 h	60
<b>12</b>	-	4	TfOH (0.5)	50 °C, 10 h	15
<b>13</b>	-	4	H <sub>2</sub> SO <sub>4</sub> -SiO <sub>2</sub> (0.5) <sup>e</sup>	50 °C, 10 h	60
<b>14</b>	-	4	Amberlyst-15 (0.5)	50 °C, 10 h	25

<sup>a</sup> 0.1 mmol of (**2a** + **2b**) [0.02 mol/L]. <sup>b</sup> Use of Dean-Stark apparatus. <sup>c</sup> Use of 3 Å molecular sieves. <sup>d</sup> Isolated yield. <sup>e</sup> H<sub>2</sub>SO<sub>4</sub>-SiO<sub>2</sub> [0.5 mmol/g].

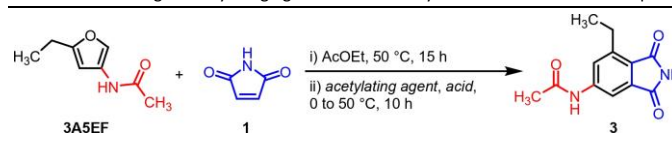
Inspired by the methodology described in the patent WO 2019/212338 A1, we tested the use of the acetylating agent acetic anhydride (Ac<sub>2</sub>O) as an additive.<sup>46a</sup> Gratifyingly, the formation of product **3** occurred with 80% yield at 50 °C under acidic conditions (Table 2, entry 7). When the reaction is carried out at 25 °C, a longer reaction time is required and the yield decreases to 70% (Table 2, entry 8). Decreasing the amount of Ac<sub>2</sub>O to 2 equivalents led to a drop in the yield to 50% (Table 2, entry 9). Use of fewer equivalents of H<sub>2</sub>SO<sub>4</sub> catalyst (0.25 equiv.) also resulted in a drop in yield to 70% (Table 2, entry 10). Other acids such as TfOH, Amberlyst-15, *p*-TsOH and H<sub>2</sub>SO<sub>4</sub>-SiO<sub>2</sub>, were also tested, but there was no improvement in the yield (Table 2, entries 11–14).

Thus, we investigated the possibility of performing the two reactions sequentially, without the requirement of purifying the DA adduct. In initial experiments, after 15 hours of reaction to form the DA adduct, methanol was removed from the medium by rotary evaporation and the process continued with the addition of Ac<sub>2</sub>O and H<sub>2</sub>SO<sub>4</sub> at 0 °C. Pleasingly, after a period of 10 hours at 50 °C, product **3** was formed in the same 80% yield.

To avoid extra unit operations, we also tested the possibility of using another solvent that did not need to be removed from the reaction medium before adding Ac<sub>2</sub>O and H<sub>2</sub>SO<sub>4</sub>. According to the data presented in Table 1c (entry 6), ethyl acetate could be a good solvent, as it promotes the DA reaction in good yield, and it is also a green solvent.<sup>46b</sup> Thus, we tested the reaction with ethyl acetate and, at the end of the process, we were able to obtain compound **3** in 80% yield for the two steps. Since best results of aromatisation were achieved using sulphuric acid, we evaluated the recyclability of H<sub>2</sub>SO<sub>4</sub>-SiO<sub>2</sub> aiming for a recoverable catalyst system, but unfortunately in the second catalytic cycle compound **3** is formed in negligible yield.

To diminish the negative environmental impact related to the use of H<sub>2</sub>SO<sub>4</sub>, we also explored alternative acids (Table 3) such as HCl, AcOH, H<sub>3</sub>PO<sub>4</sub>, MsOH and TFA, but unfortunately compound **3** was formed with low (entries 5 and 7) or trace yields (entries 2 and 3). The use of AcOH or HCl did not promote the formation of **3**, with no consumption of starting material. We also investigated the use of other greener acetylating agents to replace acetic anhydride, however only traces of compound **3** were observed. In these cases, probably acid catalysed polymerisation took place consuming the acetylating agent, even when milder acids were used. Sulfuric waste generated after reactions were properly treated by neutralization and disposed of accordingly, despite all efforts to avoid concentrated sulfuric acid and its subsequent treatment.

**Table 3** Screening of acetylating agent and acid catalyst for the aromatisation step



Entry <sup>a</sup>	Acetylating agent (4 equiv.)	Acid (0.5 equiv.)	Yield <sup>c</sup> (%)
<b>1</b>	Ac <sub>2</sub> O	H <sub>2</sub> SO <sub>4</sub>	80
<b>2</b>	Ac <sub>2</sub> O	TFA	traces
<b>3</b>	Ac <sub>2</sub> O	H <sub>3</sub> PO <sub>4</sub>	traces
<b>4</b>	Ac <sub>2</sub> O	AcOH	-
<b>5</b>	Ac <sub>2</sub> O	MsOH	12
<b>6</b>	Ac <sub>2</sub> O	HCl	-
<b>7</b>	Ac <sub>2</sub> O	H <sub>2</sub> SO <sub>4</sub> -SiO <sub>2</sub> <sup>b</sup>	30
<b>8</b>	Vinyl acetate	TFA	-
<b>9</b>	Vinyl acetate	H <sub>3</sub> PO <sub>4</sub>	-
<b>10</b>	Vinyl acetate	MsOH	traces
<b>11</b>	Vinyl acetate	H <sub>2</sub> SO <sub>4</sub> -SiO <sub>2</sub> <sup>b</sup>	traces
<b>12</b>	Vinyl acetate	H <sub>2</sub> SO <sub>4</sub>	traces
<b>13</b>	Isopropenyl acetate	TFA	-
<b>14</b>	Isopropenyl acetate	H <sub>3</sub> PO <sub>4</sub>	-
<b>15</b>	Isopropenyl acetate	MsOH	traces
<b>16</b>	Isopropenyl acetate	H <sub>2</sub> SO <sub>4</sub> -SiO <sub>2</sub> <sup>b</sup>	traces
<b>17</b>	Isopropenyl acetate	H <sub>2</sub> SO <sub>4</sub>	traces

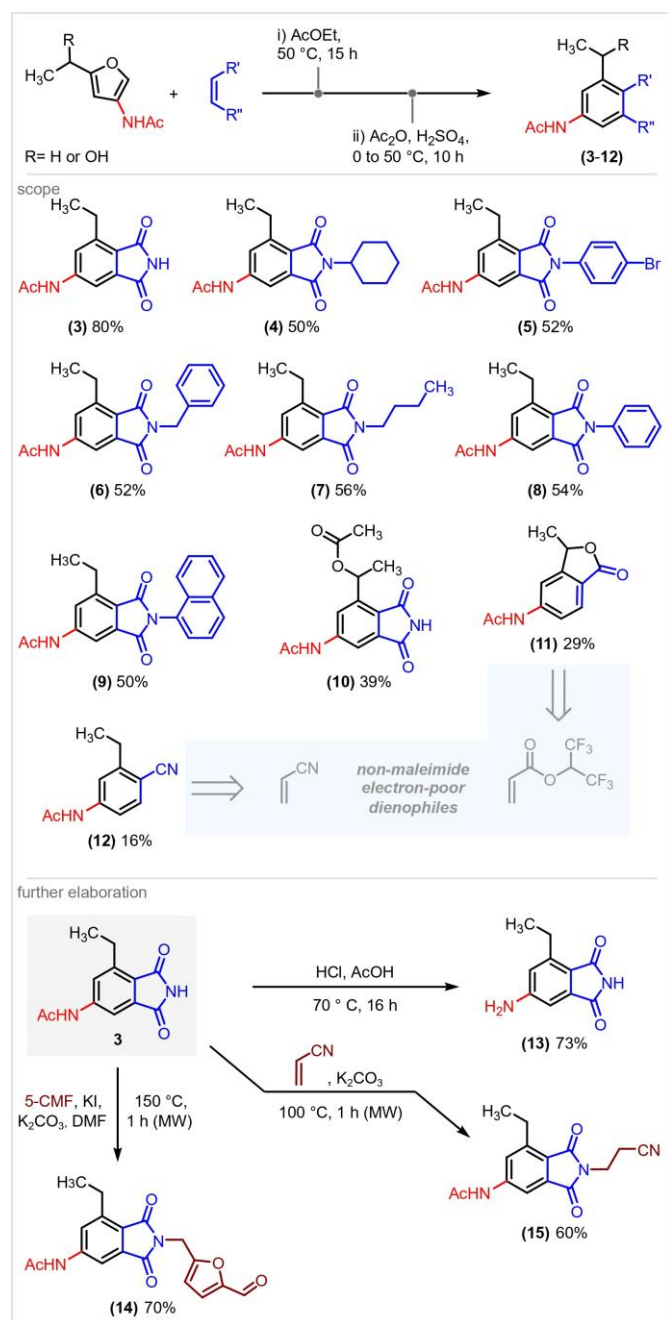
<sup>a</sup> 0.1 mmol of (**2a** + **2b**) [0.02 mol/L]. <sup>b</sup> H<sub>2</sub>SO<sub>4</sub>-SiO<sub>2</sub> [5 mmol/g]. <sup>c</sup> Isolated yield.

#### Scope of aromatics and follow-up chemistry

The scope for this newly developed two-step sequential process for the formation of phthalimides **4–9** from **3A5EF** was planned for a set of *N*-substituted maleimides with overall yield around 50%, except for model compound **3** (80%, Scheme 1).

Using **3A5HF** as diene, it was possible to obtain phthalimide **10** in 39% yield. As the reaction medium is highly acetylating, the only product obtained was compound **10**. The reaction of **3A5HF** with the dienophile 1,1,1,3,3,3-hexafluoroisopropyl acrylate provided lactone **11** in 29% yield (for three steps). In this case, the DA reaction was favoured by the dynamic trapping that led to the lactonisation of the DA adducts, since the use of other acrylates (methyl acrylate or acrylic acid) failed to give the desired product.<sup>21</sup> We were also able to obtain the acetamino benzonitrile **12** through the reaction of **3A5EF** with acrylonitrile. Despite the low yield for this reaction, the resulting compound presents a substitution pattern that is difficult to install through classic reactions involving aromatic compounds. It is important to note that in the last two examples only the *ortho*-regioisomer was isolated, in agreement with Frontier Molecular Orbital (FMO) theory considerations.





**Scheme 1** Scope of phthalimides (4–9) and aromatic compounds (11 and 12) obtained from **3A5EF** and **3A5HF**.

Afterwards, some modifications of phthalimide **3** were investigated to demonstrate the versatility of these materials (Scheme 1). Thus, deacetylation of phthalimide **3** was performed in acid medium providing the 4-amino derivative **13** in 73% yield. Phthalimide *N*-alkylation reaction was carried out with 5-chloromethylfurfural (5-CMF), obtained from fructose<sup>47</sup>, leading to the formation of the *N*-substituted compound **14** with 70% yield under microwave heating. Finally, an *aza*-Michael reaction of compound **3** with acrylonitrile afforded compound **15** with 60% yield under microwave heating.

#### Additional mechanistic studies

DFT calculations were also carried out to investigate the mechanism of the aromatisation reaction (Figure 3). In agreement with the experimental observations, the crucial role of acetic anhydride is intercepting and stabilising reactive intermediates during the aromatisation process.

After the DA cycloaddition reaction, the DA adduct promptly reacts with the H<sub>2</sub>SO<sub>4</sub> forming the oxonium ion **Exo\_1** by the protonation of its bicyclic oxygen, as experimentally evidenced. Next, ring-opening reaction takes place leading to the formation of the carbocation intermediate **Exo\_2** with hydroxyl group in opposite side of ring, from which, after formation of the double bond, gives the neutral intermediate **Exo\_3** through an exothermic process. The role of acetic anhydride is intercepting this intermediate to turn hydroxyl out into a better leaving group, by an acetylation reaction step (**TSExo34**). However, the reaction barrier for this process is computed considerable high (*ca.* 37 kcal/mol), presumably because this reaction barrier was computed using the inactivated acetic anhydride, *i.e.* when it is not protonated.

The calculations indicate that the acidic medium also is pivotal to activate the acetic anhydride, since the formation of aromatic product **3** turns out considerably more exothermic. Furthermore, Figure 3 suggests that the subsequent proton elimination in order to form the final product **3** perhaps does not undergo by unimolecular mechanism (E1), since the formation of the carbocationic intermediates, in such reaction conditions, were strongly disfavoured. Indeed, the carbocation intermediate **Exo\_6** was computed to be 50 kcal/mol higher than the neutral intermediate **Exo\_4**. Based on that, the formation of the product **3** could occur by the activation (protonation) of acetic anhydride followed by the acetylation process and releasing of acetic acid to form the **Exo\_4'**. We could not find the transition states related to these steps. However, we envisioned that the proton elimination for the formation of the aromatic product **3** could be carried out under E2 mechanism preventing the formation of disfavoured carbocationic species.

The DA adducts **2e** and **2f** formed by the reaction between **3A5AF** and **1** were also subjected to the aromatisation reaction, but the experimental conditions led to the decomposition of the DA adduct and the formation of the desired aromatic compound was not observed. Presumably, the ketone electron-withdrawing group on the 7-oxanorbornene intermediate derived from **3A5AF** hinders the dehydration reaction, which is also supported by DFT calculations (Figure 3). Indeed, the calculations illustrate the additional disadvantageous energetic condition offered by the ketone electron-withdrawing group present in the **3A5AF** in the formation of specific cationic species (see the gray structures depicted in the Figure 3; only the steps until the formation of intermediate **Exo\_2** were computed).

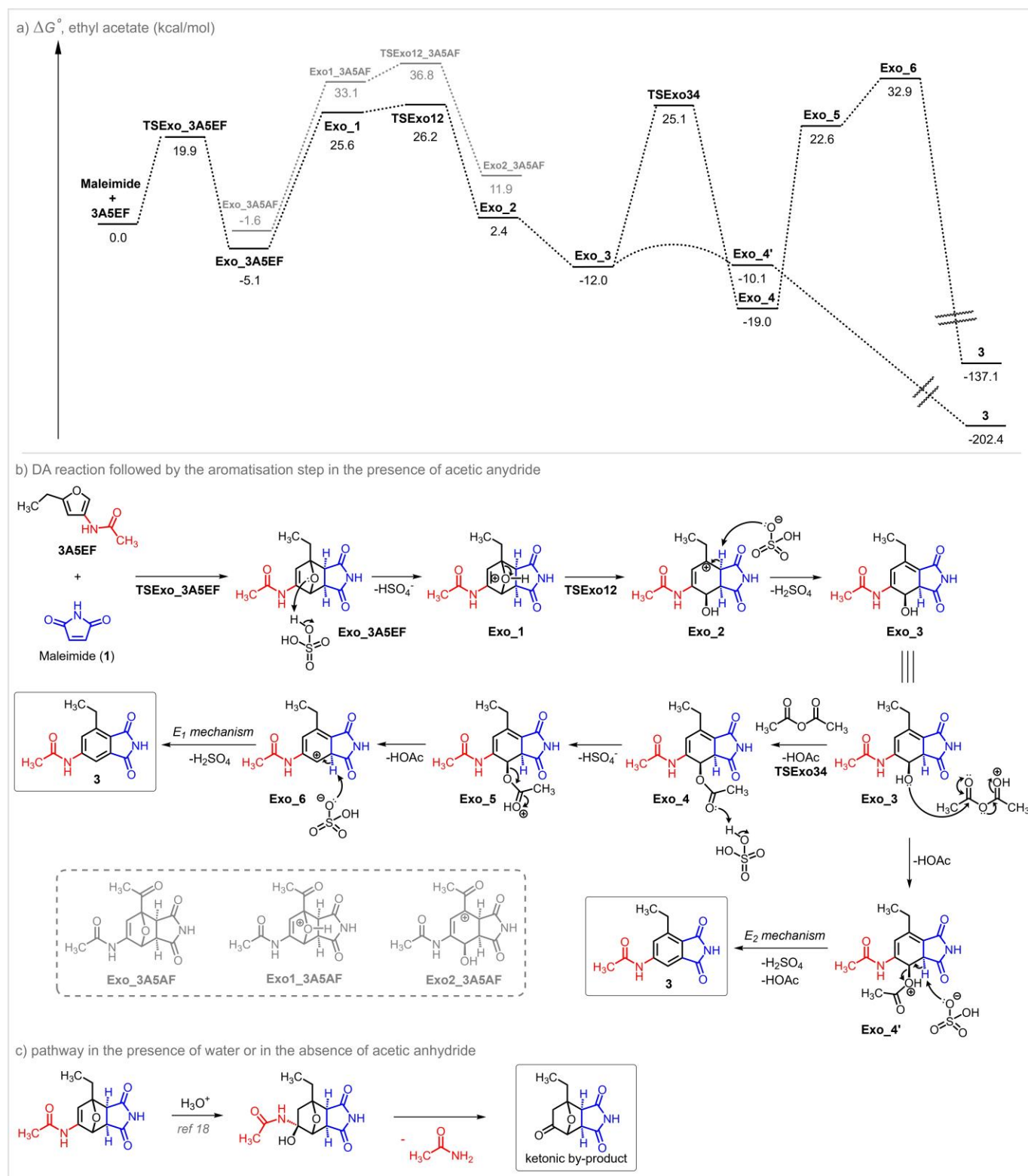


**Figure 3** DFT calculations and proposed mechanism of the aromatisation reaction. (a) Relative Gibbs free energy profiles in solution phase (ethyl acetate, kcal/mol). (b) Proposed mechanism for the aromatisation reaction highlighting the role of the acetylating agent. (c) Reaction pathway in the presence of water or in the absence of acetic anhydride.

### Fluorescence properties of 4-amino/4-acetamino-phthalimides

The 4-aminophthalimide combined with *N*-linked electron-donating groups in the phthalimide scaffold is well known to

exhibit high fluorescence. Thus, its derivatives continually attract great attention for biological applications, especially as fluorescent markers, and environment-sensitive probes.<sup>45, 48</sup>

We preliminarily investigated the photophysical properties of the compounds on exposure to UV light (Figure 4). It was noteworthy that some phthalimides **3**, **4**, **6–8** and **13–15** exhibited fluorescence when subjected to 254 and 365 nm UV light sources. Next, fluorescence analysis of compounds **3**, **4**, **6–8** and **13–15** (50  $\mu\text{M}$ , ethyl acetate) demonstrated that these compounds present emission between 400–450 nm when excited in a range of 250–460 nm. Compound **13** exhibited the highest emission intensity due to the removal of the acetyl protecting group; therefore this result paves the way for further application of 4-aminophthalimides obtained from biomass derivatives in the field of molecular fluorescence, since some 4-aminophthalimides are used as cellular biomarkers.<sup>48</sup>

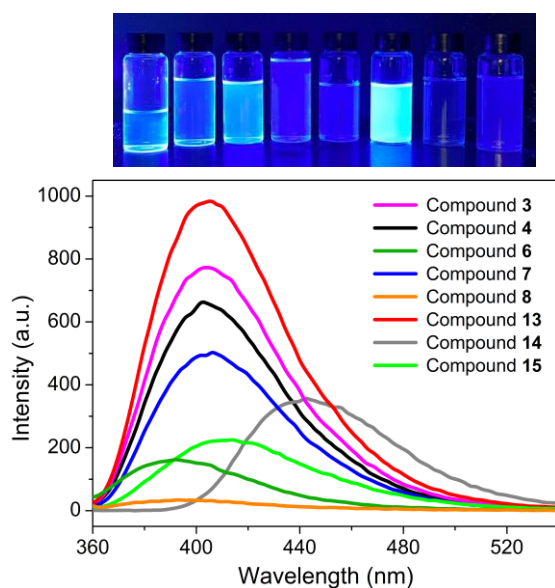


**Figure 4** Fluorescence images of compounds **3**, **4**, **6–8** and **13–15** (from left to right, respectively) in ethyl acetate at 365 nm UV light excitation (top) and emission spectra (bottom) of the solutions at 50  $\mu\text{M}$  in ethyl acetate.

## Conclusions

We demonstrated in this work the great potential of **3A5EF** and **3A5HF** as dienes in DA reactions to readily reach high-value nitrogenated aromatic compounds. The DA adducts underwent dehydration reactions as a key step leading to the synthesis of *N*-containing aromatics with the nitrogen atom directly attached to the benzene ring. Thus, we developed a unique two-step tandem process (Diels-Alder followed by aromatisation) that provides access to eight novel chitin-derived 4-acetylaminophthalimides in up to 80% yield and two *N*-containing functionalised phthalic anhydride and benzonitrile derivatives in up to 29% yield. Computational calculations suggest that the DA adduct formed from **3A5EF** and maleimide is thermodynamically favoured compared to the carbonyl-substituted adduct derived from **3A5AF**. With regards to our mechanism investigations, the **3A5AF**-derived DA adduct shows no aromatisation despite the presence of the carbonyl group. We propose that aromatisation is impracticable in **3A5AF**-derived 7-oxa-norbornene scaffold due to the strong destabilising effect of the electron-withdrawing carbonyl

substituent. On the other hand, the DA adducts obtained from **3A5EF** and **3A5HF** were feasible to the aromatisation step, although the DA reaction is still limited to extremely electron-poor dienophiles, e.g. maleimides, acrylonitrile and 1,1,1,3,3,3-hexafluoroisopropyl acrylate. Despite the reduced scope of dienophiles limited by dienes reactivity, a diverse range of different nitrogenated functionalised compounds was obtained and further synthetic elaborations were demonstrated employing acetyl removal, alkylation and Michael addition reactions. The generated products can be employed as useful precursors for a range of polysubstituted benzenes, demonstrating that nitrogen fixed in chitin derivatives can be incorporated into a variety of relevant aromatic chemical scaffolds. When considering the processes outlined in Figure 1a, the aromatic starting materials come from fossil-fuels and the nitration reaction takes place in oleum (fuming sulfuric acid) and concentrated nitric acid, and needs precise temperature control, ranging from cryogenics to high temperature. Thus, the process reported herein with sulfuric acid and acetic anhydride at 50  $^{\circ}\text{C}$  for 10 hours is a significant advance in complementing these techniques. Our findings will thus contribute to the synthesis of new aromatic compounds with high added-value from chitin, expanding the scope of dienes and dienophiles as a powerful toolbox in synthesis and potential use as cellular biomarkers.

## Author contributions

Conceptualisation, CSS, RRM, JCP and VHMS; Methodology, CSS, RRM and VHMS; Formal Analysis, VHMS; Investigation, CSS, RRM, JSB and VHMS; Resources, CSS, RRM, DLB and JCP; Writing – Original Draft, CSS, RRM, JCP and VHMS; Writing – Review & Editing, CSS, RRM, VHMS, DLB and JCP; Visualisation, CSS, RRM and JSB; Supervision, DLB and JCP; Funding Acquisition, CSS, RRM, JSB, DLB and JCP.

## Conflicts of interest

There are no conflicts to declare.

## Acknowledgements

The authors gratefully acknowledge financial support from the São Paulo Research Foundation – FAPESP (CSS, 2022/00774-5; RRM, 2019/26450-9 and 2022/03872-8; JCP, 2021/06661-5), the Brazilian National Council for Scientific and Technological Development – CNPq (JSB, 120853/2022–1; JCP, 308540/2021-2), and the Coordination for the Improvement of Higher Education Personnel – CAPES (RRM, Finance Code 001).

## References

- H-G. Franck and J. W. Stadelhofer, *Industrial Aromatic Chemistry*; Springer-Verlag Berlin, Heidelberg, 1988.
- A. Boateng, *Pyrolysis of Biomass for Fuels and Chemicals*, Academic Press, 2020.

- 3 C. Blum, D. Bunke, M. Hungsberg, E. Roelofs, A. Joas, R. Joas, M. Blepp and H. C. Stolzenberg, *Sustain. Chem. Pharm.*, 2017, **5**, 94.
- 4 (a) R. S. Varma, *Clean Technol. Environ. Policy*, 2021, **23**, 2497; (b) R. S. Varma, *ACS Sustain. Chem. Eng.*, 2019, **7**, 6458.
- 5 (a) L. Manni, O. Ghorbel-Bellaaj, K. Jellouli, I. Younes and M. Nasri, *Appl. Biochem. Biotechnol.*, 2010, **162**, 345; (b) X. Chen, S. L. Chew, F. M. Kerton and N. Yan, *Green Chem.*, 2014, **16**, 2204.
- 6 J-B. Zeng, Y-S. He, S-L. Li and Y-Z. Wang, *Biomacromolecules*, 2012, **13**, 1.
- 7 (a) G. A. F. Roberts, *Chitin Chemistry*, Red Globe Press, London, 1992; (b) D. Elieh-Ali-Komi and M. R. Hamblin, *Int. J. Adv. Res. (Indore)*, 2016, **4**, 411.
- 8 (a) H. Amiri, M. Aghbashlo, M. Sharma, J. Gaffey, L. Manning, S. M. M. Basri, J. F. Kennedy, V. K. Gupta and M. Tabatabaei, *Nat. Food*, 2022, **3**, 822; (b) M. Yadav, P. Goswami, K. Paritosh, M. Kumar, N. Pareek and V. Vivekanand, *Bioresour. Bioprocess.*, 2019, **6**, 8; (c) B. T. Iber and N. A. Kasan, *Heliyon*, 2021, **7**, e08283.
- 9 A. Percot, C. Viton and A. Domard, *Biomacromolecules*, 2003, **4**, 12.
- 10 V. L. Pachapur, K. Guemiza, T. Rouissi, S. J. Sarma and S. K. Brar, *J. Chem. Technol. Biotechnol.*, 2016, **91**, 2331.
- 11 H. D. de Holanda and F. M. Netto, *Food Chem. Toxicol.*, 2006, **71**, C298.
- 12 (a) K. Techikawara, H. Kobayashi and A. Fukuoka, *ACS Sustain. Chem. Eng.*, 2018, **6**, 12411; (b) H. Kobayashi, K. Techikawara and A. Fukuoka, *Green Chem.*, 2017, **19**, 3350; (c) L. Liu, *Green Chem.*, 2021, **23**, 9800; (d) K. W. Omari, L. Dodot and F. M. Kerton, *ChemSusChem.*, 2012, **5**, 1767; (e) D. Padovan, H. Kobayashi and A. Fukuoka, *ChemSusChem.*, 2020, **13**, 3594; (f) M. W. Drover, K. W. Omari, J. N. Murphy and F. M. Kerton, *RSC Adv.*, 2012, **2**, 4642.
- 13 M. J. Hülsey, H. Yang and N. Yan, *ACS Sustain. Chem. Eng.*, 2018, **6**, 5694.
- 14 A. D. Sadiq, X. Chen, N. Yan and J. Sperry, *ChemSusChem.*, 2018, **11**, 532.
- 15 T. T. Pham, A. C. Lindsay, S-W. Kim, L. Persello, X. Chen, N. Yan and J. Sperry, *ChemistrySelect*, 2019, **4**, 10097.
- 16 (a) T. T. Pham, X. Chen, T. Söhnle, N. Yan and J. Sperry, *Green Chem.*, 2020, **22**, 1978; (b) T. T. Pham, A. C. Lindsay, X. Chen, G. Gözaydin, N. Yan and J. Sperry, *Sustain. Chem. Pharm.*, 2019, **13**, 100143.
- 17 Y. Liu, C. Stähler, J. N. Murphy, B. J. Furlong and F. M. Kerton, *ACS Sustain. Chem. Eng.*, 2017, **5**, 4916.
- 18 J. G. Pereira, J. M. J. M. Ravasco, J. R. Vale, F. Queda and R. F. A. Gomes, *Green Chem.*, 2022, **24**, 7131.
- 19 J. M. J. M. Ravasco and R. F. A. Gomes, *ChemSusChem.*, 2021, **14**, 3047.
- 20 R. C. Cioc, M. Lutz, E. A. Pidko, M. Crockatt, J. C. van der Waal and P. C. A. Bruijninx, *Green Chem.*, 2021, **23**, 367.
- 21 C. S. Lancefield, B. Fölker, R. C. Cioc, K. Stanciakova, R. E. Buló, M. Lutz, M. Crockatt and P. C. A. Bruijninx, *Angew. Chem. Int. Ed.*, 2020, **59**, 23480.
- 22 R. C. Cioc, M. Crockatt, J. C. van der Waal and P. C. A. Bruijninx, *Angew. Chem. Int. Ed.*, 2022, **61**, e202114720.
- 23 I. van Scodeller, K. O. Vigier, E. Muller, C. Ma, F. Guégan, R. Wischert and F. Jérôme, *ChemSusChem.*, 2021, **14**, 313.
- 24 S. Higson, F. Subrizi, T. D. Sheppard and H. C. Hailes, *Green Chem.*, 2016, **18**, 1855.
- 25 L. Ni, J. Xin, K. Jiang, L. Chen, D. Yan, X. Lu and S. Zhang, *ACS Sustain. Chem. Eng.*, 2018, **6**, 2541.
- 26 J. K. Ogunjobi, T. J. Farmer, C. R. McElroy, S. W. Breeden, D. J. Macquarrie, D. Thornthwaite and J. H. Clark, *ACS Sustain. Chem. Eng.*, 2019, **7**, 8183.
- 27 X. Li, X. Ma, Z. Wang, P-N. Liu and L. Zhang, *Angew. Chem. Int. Ed.*, 2019, **58**, 17180.
- 28 E. Mahmoud, D. A. Watson and R. F. Lobo, *Green Chem.*, 2014, **16**, 167.
- 29 J. A. M. Mesa, F. Brandi, I. Shekova, M. Antonietti and M. Al-Naji, *Green Chem.*, 2020, **22**, 7398.
- 30 S. Thiyagarajan, H. C. Genuino, M. Šliwa, J. C. van der Waal, E. de Jong, J. van Haveren, B. M. Weckhuysen, P. C. A. Bruijninx and D. S. van Es, *ChemSusChem.*, 2015, **8**, 3052.
- 31 H. C. Genuino, S. Thiyagarajan, J. C. van der Waal, E. de Jong, J. van Haveren, D. S. van Es, B. M. Weckhuysen and P. C. A. Bruijninx, *ChemSusChem.*, 2017, **10**, 277.
- 32 K. Fukui, T. Yonezawa and H. Shingu, *J. Chem. Phys.*, 1952, **20**, 722.
- 33 C-C. Chang, H. J. Cho, J. Yu, R. J. Gorte, J. Gulbinski, P. Dauenhauer and W. Fan, *Green Chem.*, 2016, **18**, 1368.
- 34 I. F. Teixeira, B. T. W. Lo, P. Kostetsky, M. Stamatakis, L. Ye, C. C. Tang, G. Mpourmpakis and S. C. E. Tsang, *Angew. Chem. Int. Ed.*, 2016, **55**, 13061.
- 35 S. Thiyagarajan, H. C. Genuino, J. C. van der Waal, E. de Jong, B. M. Weckhuysen, J. van Haveren, P. C. A. Bruijninx and D. S. van Es, *Angew. Chem. Int. Ed.*, 2016, **55**, 1368.
- 36 A. D. Pehere, S. Xu, S. K. Thompson, M. A. Hillmyer and T. R. Hoye, *Org. Lett.*, 2016, **18**, 2584.
- 37 F.A. Kucherov, K. I. Galkin, E. G. Gordeev and V. P. Ananikov, *Green Chem.*, 2017, **19**, 4858.
- 38 I. van Scodeller, S. Mansouri, D. Morvan, E. Muller, K. O. Vigier, R. Wischert, F. Jérôme, *Angew. Chem. Int. Ed.*, 2018, **57**, 10510.
- 39 R. C. Cioc, T. J. Smak, M. Crockatt, J. C. van der Waal and P. C. A. Bruijninx, *Green Chem.*, 2021, **23**, 5503.
- 40 (a) F. A. Kucherov, L. V. Romashov, G. M. Averochkin and V. P. Ananikov, *ACS Sustain. Chem. Eng.*, 2021, **9**, 3011; (b) J. He, L. Chen, S. Liu, K. Song, S. Yang and A. Riisager, *Green Chem.*, 2020, **22**, 6714.
- 41 E. Vitaku, D. T. Smith and J. T. J. Njardarson, *J. Med. Chem.*, 2014, **57**, 10257.
- 42 X. Zhang, E. A. Davidson, D. L. Mauzerall, T. D. Searchinger, P. Dumas and Y. Shen, *Nature*, 2015, **528**, 51.
- 43 (a) N. Yan and X. Chen, *Nature*, 2015, **524**, 155; (b) M. J. Hülsey, H. Yang and N. Yan, *ACS Sustain. Chem. Eng.*, 2018, **6**, 5694; (c) T. M. Lammens, M. C. R. Franssen, E. L. Scott and J. P. M. Sanders, *Biomass Bioenergy*, 2012, **44**, 168; (d) M. B. A. Kumar, Y. Gao, W. Shen and L. He, *Front. Chem. Sci. Eng.*, 2015, **9**, 295; (e) S-Y. Li, I-S. Ng, P. T. Chen, C-J. Chiang and Y-P. Chao, *Biotechnol. Biofuels*, 2018, **11**, 256.
- 44 M. Weinberger, F. Berndt, R. Mahrwald, N. P. Ernsting and H-A. Wagenknecht, *J. Org. Chem.*, 2013, **78**, 2589.
- 45 J. Riedl, R. Pohl, N. P. Ernsting, P. Orság, M. Fojta and M. Hocek, *Chem. Sci.*, 2012, **3**, 2797.
- 46 (a) N. Crockatt and J. Urbanus, *Diels-Alder Ring-opening Process*, WO 2019/212338 A1, 2019; (b) R. K. Henderson, C. Jiménez-González, D. J. C. Constable, S. R. Alston, G. G. A. Inglis, G. Fisher, J. Sherwood, S. P. Binks and A. D. Curzons, *Green Chem.*, 2011, **13**, 854.
- 47 N. Kumari, J. K. Olesen, C. M. Pedersen and M. Bols, *Eur. J. Org. Chem.*, 2011, **2011**, 1266.
- 48 S. Shahbazi, C. J. Peer, M. N. Polizzotto, T. S. Uldrick, J. Roth, K. M. Wyvill, K. Aleman, J. B. Zeldis, R. Yarchoan and W. D. Figg, *J. Pharm. Biomed. Anal.*, 2014, **92**, 63.